International Journal on "Technical and Physical Problems of Engineering" (IJTPE)
Published by International Organization on TPE (IOTPE)
ISSN 2077-3528
IJTPE Journal
www.iotpe.com
ijtpe@iotpe.com

December 2011	Issue 9	Volume 3	Number 4	Pages 59-67

SVD-UPFC BASED DESIGNATION OF VERSATILE CONTROLLERS TO DAMP LOW FREQUENCY OSCILLATIONS

N.M. Tabatabaei [1,2] A. Demiroren [2] N. Taheri [3] A. Hashemi [4] N.S. Boushehri [1]

1. Electrical Engineering Department, Seraj Higher Education Institute, Tabriz, Iran
n.m.tabatabaei@gmail.com, nargesboush@yahoo.com
2. Electrical Engineering Department, Faculty of Electrical and Electronic Engineering,
Istanbul Technical University, Maslak, Istanbul, Turkey, demiroren@itu.edu.tr
3. Electrical Engineering Department, Islamic Azad University, Quchan Branch, Quchan, Iran
n.taheri.1362@gmail.com
4. Electrical Engineering Department, Sama Technical and Vocational College,
Islamic Azad University, Kermanshah Branch, Kermanshah, Iran, ahmad.hashemi.v@gmail.com

Abstract- Unified power flow controller (UPFC) is the most reliable device in the FACTS concept. It has the ability to adjust all three control parameters effective in power flow and voltage stability. In this paper, a linearized model of a power system installed with a UPFC has been presented. UPFC has four control loops that, by adding an extra signal to one of them, increases dynamic stability and load angle oscillations are damped. In this paper, after open loop eigenvalue (electro mechanical mode) calculations, state-space equations has been used to design damping controllers and it has been considered to influence active and reactive power flow durations as the input of damping controllers, in addition to the common speed duration of synchronous generators as input damper signals. SVD controllability measurements determine the most effective control input to apply to the system. Dynamic stability has been improved via Lead-Lag and LQR controllers' designation.

Keywords: UPFC, State-Space Equations, SVD, LQR.

I. INTRODUCTION

Power transfer in an integrated power system is constrained by transient stability, voltage stability and small signal stability. These constraints limit a full utilization of available transmission corridors. The flexible AC transmission system (FACTS) is the technology that provides the needed corrections of the transmission functionality in order to fully utilize the existing transmission facilities and hence, minimizing the gap between the stability limit and thermal limit [1].

A unified power flow controller (UPFC) is one the FACTS devices which can control power system parameters such as terminal voltage, line impedance and phase angle [2]. Recently, researchers have presented dynamic UPFC models in order to design a suitable controller for power flow, voltage and damping controls [9-17]. Wang has presented a modified linearized Heffron-Phillips model of a power system installed with a UPFC [1, 3, 7, 11] but no effort seems to have been made to identify the most suitable UPFC control parameters, in order to arrive at a robust damping controller and has not used the deviation of active and reactive powers, ΔP_e and ΔQ_e as the input control signals.

The ΔP_e and ΔQ_e signals can be used for oscillation damping as input signals due to their improved convenience over $\Delta\omega$ especially in states where UPFCs are set too far from the generator. In this paper, the dynamic equations of ΔQ_e has been calculated and has been used from the deviations signals of active and reactive power and their sum, and also rotor speed deviation as input control signals for Lead-Lag controllers and their results have been compared with each other.

In addition, it has examined the relative effectiveness of modulating alternative UPFC control parameters m_E, m_B, δ_E and δ_B for damping power system oscillations via the SVD technique. Additionally, it has designed two kinds of power controllers including Lead-Lag, LQR for power systems installed with UPFC and their effects has been compared for damping the power system oscillations.

II. THE POWER SYSTEM CASE STUDY

Figure 1 shows a single-machine-infinite-bus (SMIB) system installed with UPFC. The static excitation system model type IEEE-ST1A has been considered. The UPFC considered here is assumed to be based on pulse width modulation (PWM) converters.

The UPFC is a combination of a static synchronous compensator (STATCOM) and a static synchronous series compensator (SSSC) which are coupled via a common dc link, to allow bi-directional flow of real power between the series output terminals of the SSSC and the shunt output terminals of the STATCOM, and are controlled real and reactive series line compensations without an external electric energy source.

The UPFC, by means of angularly unconstraint series voltage injection, is able to control, concurrently or selectively, the transmission line voltage, impendence and angle or alternatively, the real and reactive power flow in the line. The UPFC may also provide independently controllable shunt reactive compensation.

Viewing the operation of the UPFC from the stand point of conventional power transmission based on reactive shunt compensation, series compensation and phase shifting, the UPFC can fulfill all these functions and thereby meet multiple control objectives by adding the injected voltage V_{Bt} with appropriate amplitude and phase angle, to the terminal voltage V_{Et}.

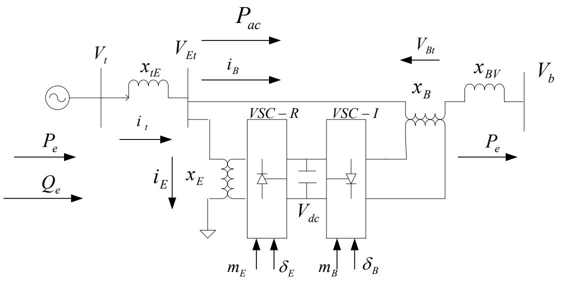

Figure 1. UPFC installed in a SMIB system

III. STATE SPACE EQUATIONS OF POWER SYSTEM

If the general pulse width modulation (PWM) is adopted for GTO-based VSCs, the three-phase dynamic differential equations of the UPFC are [6]:

$$\Delta\dot{\delta} = \omega_b \Delta\omega$$
$$\Delta\dot{\omega} = \frac{\Delta P_m - \Delta P_e - D\Delta\omega}{M}$$
$$\Delta\dot{E}'_q = \frac{-\Delta E_q + \Delta E_{fd} + (x_d - x'_d)\Delta i_d}{T'_{do}}$$
$$\Delta\dot{E}_{fd} = \frac{-\Delta E_{fd} + K_A(\Delta V_{ref} - \Delta v + \Delta u_{PSS})}{T_A} \quad (1)$$
$$\Delta\dot{V}_{dc} = K_7\Delta\delta + K_8\Delta E'_q - K_9\Delta V_{dc} +$$
$$K_{ce}\Delta m_E + K_{c\delta e}\Delta\delta_E + K_{cb}\Delta m_B + K_{c\delta b}\Delta\delta_B$$

The equations below can be obtained with a line arising from Equation (1).

$$\Delta P_e = K_1\Delta\delta + K_2\Delta E'_q + K_{qd}\Delta V_{dc} + $$
$$+K_{qe}\Delta m_E + K_{q\delta e}\Delta\delta_E + K_{qb}\Delta m_B + K_{q\delta b}\Delta\delta_B \quad (2)$$

$$\Delta E'_q = K_4\Delta\delta + K_3\Delta E'_q + K_{qd}\Delta V_{dc} + $$
$$+K_{qe}\Delta m_E + K_{q\delta e}\Delta\delta_E + K_{qb}\Delta m_B + K_{q\delta b}\Delta\delta_B \quad (3)$$

$$\Delta V_t = K_5\Delta\delta + K_6\Delta E'_q + K_{vd}\Delta V_{dc} + $$
$$+K_{ve}\Delta m_E + K_{v\delta e}\Delta\delta_E + K_{vb}\Delta m_B + K_{v\delta b}\Delta\delta_B \quad (4)$$

$$\Delta V_{dc} = K_7\Delta\delta + K_8\Delta E'_q - K_9\Delta V_{dc} + $$
$$+K_{ce}\Delta m_E + K_{c\delta e}\Delta\delta_E + K_{cb}\Delta m_B + K_{c\delta b}\Delta\delta_B \quad (5)$$

The state-space equations of the system can be calculated by combination of Equations (2) to (5) with Equation (1):

$$\dot{x} = Ax + Bu$$
$$x = [\Delta\delta, \Delta\omega, \Delta E'_q, \Delta E_{fd}, \Delta V_{dc}]^T \quad (6)$$
$$u = [\Delta u_{pss}, \Delta m_E, \Delta\delta_E, \Delta m_B, \Delta\delta_B]^T$$

where Δm_E, Δm_B, $\Delta\delta_E$ and $\Delta\delta_B$ are a linearization of the input control signal of the UPFC and the equations related to the K parameters have been presented in Appendix 3 [17]. The linearized dynamic model of Equations (2) to (5) can be seen in Figure 2, where there is only one input control signal for Δu. Figure 2 includes the UPFC relating the pertinent variables of electric torque, speed, angle, terminal voltage, field voltage, flux linkages, UPFC control parameters and dc link voltage.

$$A = \begin{bmatrix} 0 & \omega_b & 0 & 0 & 0 \\ -\frac{K_1}{M} & -\frac{D}{M} & -\frac{K_2}{M} & 0 & -\frac{K_{pd}}{M} \\ -\frac{K_4}{M} & 0 & -\frac{K_3}{T'_{do}} & \frac{1}{T'_{do}} & -\frac{K_{qd}}{T'_{do}} \\ -\frac{K_A K_5}{T_A} & 0 & -\frac{K_A K_6}{T_A} & -\frac{1}{T_A} & -\frac{K_A K_{pd}}{T_A} \\ K_7 & 0 & K_8 & 0 & -K_9 \end{bmatrix} \quad (7)$$

$$B = \begin{bmatrix} 0 & 0 & 0 & 0 & 0 \\ 0 & -\frac{K_{pe}}{M} & -\frac{K_{p\delta e}}{M} & -\frac{K_{pb}}{M} & -\frac{K_{p\delta b}}{M} \\ 0 & -\frac{K_{qe}}{T'_{do}} & -\frac{K_{q\delta e}}{T'_{do}} & -\frac{K_{qb}}{T'_{do}} & -\frac{K_{q\delta b}}{T'_{do}} \\ \frac{K_A}{T_A} & -\frac{K_A K_{ve}}{T_A} & -\frac{K_A K_{v\delta e}}{T_A} & -\frac{K_A K_{vb}}{T_A} & -\frac{K_A K_{v\delta b}}{T_A} \\ 0 & K_{ce} & K_{c\delta e} & K_{cb} & K_{c\delta b} \end{bmatrix}$$

A. Operating Points Calculating in Steady Condition

The primary d-q based axis of voltage, current and load angle of the system, necessary for K parameters calculating in Equation (7), have been obtained for the three conditions shown below:

- Case A: light operating condition:

$$P_e = 0.2 \text{ pu}, \; Q_e = 0.01 \text{ pu} \quad (8)$$

- Case B: nominal operating condition:

$$P_e = 0.8 \text{ pu}, \; Q_e = 0.167 \text{ pu} \quad (9)$$

- Case C: heavy operating condition:

$$P_e = 1.2 \text{ pu}, \; Q_e = 0.4 \text{ pu} \quad (10)$$

Step 1: First, by solving the four equations below, we compute the parameters V_{td}, V_{tq}, i_{td} and i_{tq} at every operating condition.

$$V_{td}^2 + V_{tq}^2 = 1 \quad (11)$$
$$V_{td} i_{td} + V_{tq} i_{tq} = P_e \quad (12)$$
$$V_{td} i_{tq} - V_{tq} i_{td} = Q_e \quad (13)$$
$$V_{td} = x_q i_{tq} \quad (14)$$

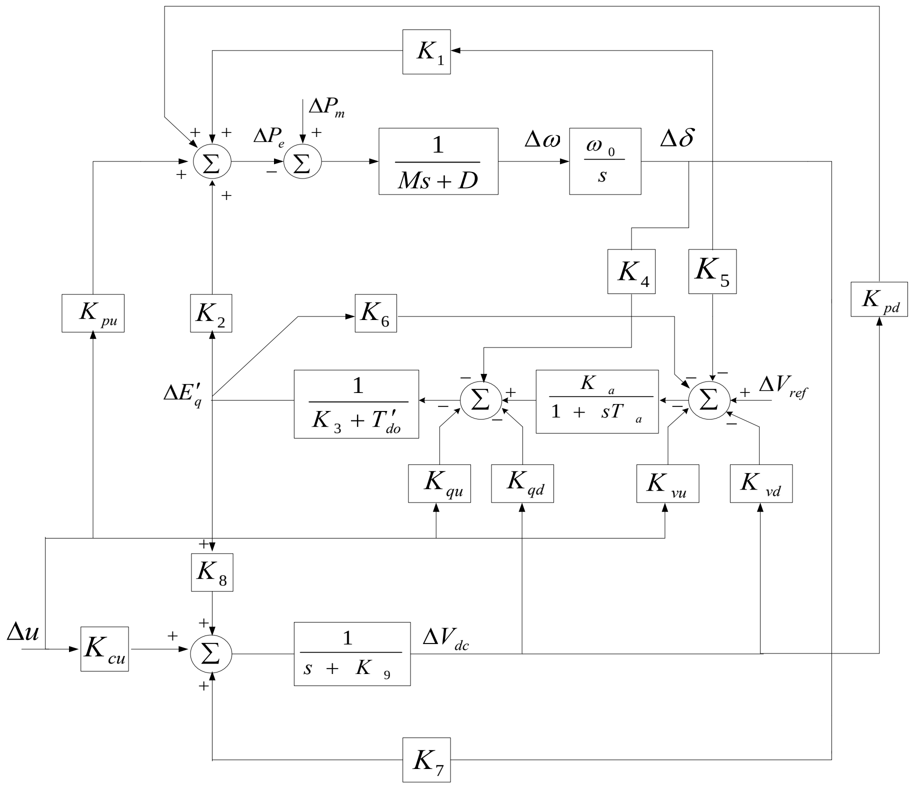

Figure 2. Modified Heffron-Phillips model of SMIB system with UPFC

Step 2: By solving the 10 equations below, parameters V_{Etd}, V_{Etq}, V_{bd}, V_{bq}, i_{Bd}, i_{Bq}, V_{Btd}, V_{Btq}, i_{Ed} and i_{Eq} will be obtained:

$$
\begin{aligned}
&V_{bd}^2+V_{bq}^2=1\\
&V_{Etd}i_{Bd}+V_{Etq}i_{Bq}=P_{ac}\\
&V_{Etd}=-(x_B+x_{BV})i_{Bq}-V_{Bd}+V_{bd}\\
&V_{Etq}=(x_B+x_{BV})i_{Bd}-V_{Bq}+V_{bq}\\
&V_{Bd}i_{Bd}+V_{Bq}i_{Bq}=P_{dc}\\
&V_{Etd}i_{Ed}+V_{Etq}i_{Eq}=P_{dc}\\
&V_{Ed}=V_{Etd}+x_Ei_{Eq}\\
&V_{Eq}=V_{Etq}-x_Ei_{Ed}
\end{aligned}
\tag{15}
$$

B. ΔQ_e Calculation

In this section, the dynamic equations relevant to the reactive power deviations will be calculated for use as the input damping control signal. According to Figure 1, the following equations can be written:

$$Q_e=V_{td}i_{tq}-V_{tq}i_{td} \tag{16}$$

$$V_{tq}=E'_q-x'_di_{td} \tag{17}$$

$$V_{td}=x_qi_{tq} \tag{18}$$

$$Q_e=(x_qi_{tq})i_{tq}-(E'_q-x'_di_{td})i_{td} \tag{19}$$

Dynamic d-q based equations of currents relevant to the reference system can be obtained as follows:

$$
\begin{aligned}
i_{Ed}=&\frac{X_{BB}}{X_{d\Sigma}}E'_q-\frac{m_E\sin\delta_EV_{dc}X_{Bd}}{2X_{d\Sigma}}+\\
&+\frac{X_{dE}}{X_{d\Sigma}}(V_b\cos\delta+\frac{m_B\sin\delta_BV_{dc}}{2})
\end{aligned}
\tag{20}
$$

$$
\begin{aligned}
i_{Eq}=&\frac{m_E\cos\delta_EV_{dc}X_{Bq}}{2X_{q\Sigma}}-\\
&-\frac{X_{qE}}{X_{q\Sigma}}(V_b\sin\delta+\frac{m_B\cos\delta_BV_{dc}}{2})
\end{aligned}
\tag{21}
$$

$$
\begin{aligned}
i_{Bd}=&-\frac{X_{dt}}{X_{d\Sigma}}(V_b\cos\delta+\frac{m_B\sin\delta_BV_{dc}}{2})-\\
&-\frac{X_{dE}}{X_{d\Sigma}}\frac{m_E\sin\delta_EV_{dc}}{2}+\frac{X_E}{X_{d\Sigma}}E'_q
\end{aligned}
\tag{22}
$$

$$
\begin{aligned}
i_{Bq}=&-\frac{X_{qt}}{X_{q\Sigma}}(V_b\sin\delta+\frac{m_B\cos\delta_BV_{dc}}{2})-\\
&-\frac{X_{qE}}{X_{q\Sigma}}\frac{m_E\cos\delta_EV_{dc}}{2}
\end{aligned}
\tag{23}
$$

ΔQ_e Signal can be assumed as Equation (24):

$$
\begin{aligned}
\Delta Q_e=&K_{10}\Delta\delta+K_{11}\Delta E'_q+K_{12}\Delta V_{dc}+K_{13}\Delta m_E+\\
&+K_{14}\Delta\delta_E+K_{15}\Delta m_B+K_{16}\Delta\delta_B
\end{aligned}
\tag{24}
$$

From Equations (19) to (23) in comparison with Equation (24) the *K*-constant values can be calculated as Appendix 2.

C. Singular Value Decomposition

Singular value decomposition (SVD) is employed to measure the controllability of the Electro Mechanical mode (EM mode) from each of the four inputs: (m_E, m_B, δ_E and δ_B) [4, 6]. The minimum singular value $\sigma_{\min}$, is estimated over a wide range of operating conditions ($P_e : [0.05 \ \rightarrow \ 1.5]$ and $Q_e : [-0.4 \ \rightarrow \ 0.4]$ pu).

SVD produces a non-negative diametric matrix (S) with dimensions of $n \times n$ and it creates unitary U and V matrixes as below:

$$x = U * S * V \quad , \quad [U, S, V] = \text{svd}(x) \tag{25}$$

Figure 3 shows the $\sigma_{\min}$ for all four inputs at $Q_e = 0.4$ pu. According to Figure 3, it can be seen that the EM mode controllability with δ_E is more than other inputs and is the least affected by loading conditions.

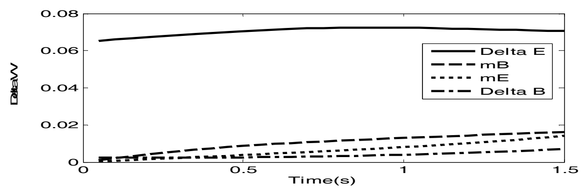

Figure 3. Minimum singular value with all inputs at $Q_e = 0.4$ pu

IV. DESIGN OF DAMPING CONTROLLERS

A. Lead-Lag Controller

The damping controllers are designed to produce an electrical torque in phase with the speed deviation. The four control parameters of the UPFC (i.e., m_E, m_B, δ_E and δ_B) can be modulated in order to produce the damping torque. The speed deviation $\Delta\omega$ is considered as the input to the damping controllers. The structure of the UPFC based damping controller is shown in Figure 4. It consists of gain, signal washout and phase compensator blocks. The parameters of the damping controller are obtained using the phase compensation technique [12]. According to Figure 4, the structures of Lead-Lag controllers with $\Delta\omega$ and ΔP_e inputs are very similar.

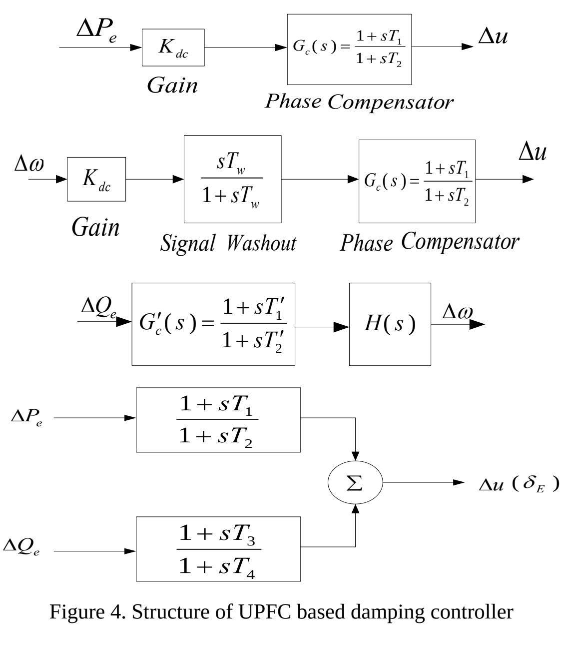

Figure 4. Structure of UPFC based damping controller

The detailed step-by-step procedure for computing the parameters of the damping controllers using the phase compensation technique is given below. At first, the natural frequency of oscillations ω_n is calculated for the mechanical loop.

$$\omega_n = \sqrt{\frac{K_1 \omega_0}{M}} \tag{26}$$

where the amounts of ω_0, K_1 and M has been presented in Appendix 1. For computing the phase lag between Δu and ΔP_e at $s = j\omega_n$, we should calculate the transfer function of Figure 5, which is a simple control model of Figure 5. The phase Lead-Lag compensator G_C is designed to provide the required degree of phase compensation for 100% phase compensation.

$$\angle G_C(j\omega) + \angle \gamma(j\omega) = 0 \tag{27}$$

Assuming one Lead-Lag network, $T_1 = aT_2$ the transfer function of the phase compensator becomes,

$$G_C(s) = \frac{1 + saT_2}{1 + sT_2} \tag{28}$$

Since the phase angle compensated by the Lead-Lag network is equal to $-\gamma$, the parameters a and T_2 are computed as,

$$a = \frac{1 + \sin\gamma}{1 + \sin\gamma}, \qquad T_2 = \frac{1}{\omega_n \sqrt{a}} \tag{29}$$

The require gain setting K_{dc} for desired value of damping ratio $\xi = 0.5$ is obtained as,

$$K_{dc} = \frac{2\xi\omega_n M}{|G_C(s)||\gamma(s)|} \tag{30}$$

and $|G_C(s)|$ and $|\gamma(s)|$ are computed at $s = j\omega_n$.

The signal washout is the high pass filter that prevents steady changes in the speed from modifying the UPFC input parameter. The value of the washout time constant T_W should be high enough to allow signals associated with oscillations in rotor speed to pass unchanged. From the view point of the washout function, the value of T_W is not critical and may be in the range of 1s to 20s.

T_W equal to 10s is chosen in the present studies. Figure 6 shows the transfer function of the system relating the electrical component of the power ΔP_{EM} produced by the damping controller δ_E.

In order to design a controller with ΔQ_e input signal for damping signal δ_E, transfer function $H(s) = \frac{\Delta Q_e}{\Delta\omega}$ must be calculated according to Equation (24) as shown below:

$$H(s) = \frac{\Delta Q_e}{\Delta\omega} = \frac{K_{10}H_{12} + K_{11}H_{32} + K_{12}H_{52} + K_{14}}{H_{22}} \tag{31}$$

So it can be obtained:

$$\angle \Delta Q_e = \angle H(s) + \angle \Delta\omega \tag{32}$$

Therefore, the compensator Lead-Lag controller $G'_C(s)$ must be designed to compensate for the phase shifting between ΔQ_e and $\Delta\omega$. The transfer function between ΔQ_e and $\Delta\omega$ according to Equation (24), has been calculated as Equation (31). For design damping controller with input $\Delta P_e + \Delta Q_e$, two Lead-Lag compensators must compensate for the phase angle between Δu and ΔP_{EM} together.

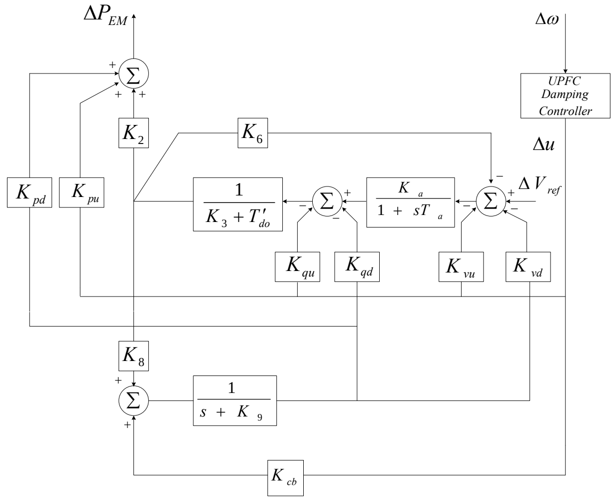

Figure 5. Transfer function of the system relating component of electrical power ΔP_{EM} produced by damping controller δ_E

B. LQR Controller

The LQR controller for a system described with the state-feedback equation $\dot{x} = Ax + B$ can calculate the optimal amount of K so that the state feedback $u = -Kx$ according to Figure 6 to minimize the integral of Equation (34).

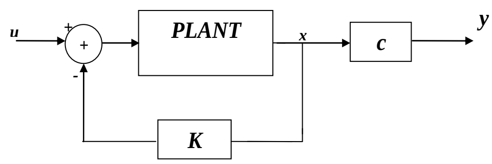

Figure 6. Block diagram of a state-space based system with negative feedback

$$J(u) = \int_0^\infty (x^T Qx + u^T Ru + 2x^T Nu)dt \quad (33)$$

In addition to calculating the optimal value of *K*, the LQR calculates the solution *S* of the associated Riccati equation according to Equation (34).

$$A^T s + sA - (sB + N)R^{-1}(B^T s + N^T) + Q = 0 \quad (34)$$

The eigenvalues of closed-loop system $e = \text{eig}(A - B * K)$ is calculated, too. Note that the value of K is calculated using the response of the Riccati equation according to Equation (35).

$$K = R^{-1}(B^T s + N^T)$$
$$[K, s, e] = \text{LQR}(A, B, Q, R, N) \quad (35)$$

V. SIMULATION RESULTS

Eigen-value (electro mechanical mode) calculations should be done before any controller designing. Table 1 shows the electro mechanical mode of the system without any controller, equipped with Lead-Lag, LQR. Based on the above table, pole placement of the closed loop system equipped with controllers has improved in comparison with open loop systems. The linearized models of the case study system in Figure 1 with parameters are shown in Appendix 1 and have been simulated with MATLAB/ SIMULINK. In order to examine the robustness of the damping controllers to a step load perturbation, it has been applied a step duration in mechanical power (i.e., $e = \text{eig}(A - B^* K)$) to the system seen in Figure 2. Consequently, the reference system has four inputs; the damping input signal in Figure 3 has been added to the most effective input δ_E calculated by the SVD technique. Figure 7 shows the dynamic responses of $\Delta\omega$ with different operating conditions by Lead-Lag controller for δ_E input control signal.

Table 1. Electromechanical mode of the individual terms at *B*-condition

Without controller	$0.1052 \pm j2.8455$			
Lead-Lag	δ_E	m_E	δ_B	m_B
	$-1.780 \pm j2.7446$	$-0.46 \pm j2.9$	$-1.4187 \pm j7276$	$3.3661 \pm j1.3204$
LQR	$-0.417 \pm j2.9290$			

It is clearly seen that the dynamic performance at a heavy condition is better significantly compared to that obtained at light and nominal loadings because the speed deviation has been damped with minimum settling time at a heavy condition. The response of the nominal condition has the second rank after the heavy condition because its settling time is less than five seconds and its peak amplitude value is even greater than the heavy condition.

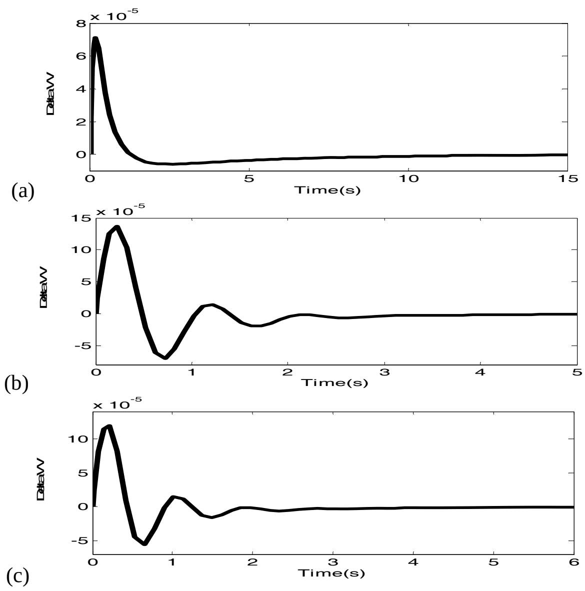

Figure 7. Dynamic responses of $\Delta\omega$ with input control signal δ_E for different operating conditions
(a) Light load (b) Nominal load (c) Heavy load

According to the above, it can be calculated by dynamic responses to the $\Delta P_m = 0.01$ pu perturbation for other input control signals that by comprising all of the responses, we can see that adding the damping control signal to δ_E is better than other control inputs because of its speed oscillation damp with a shorter time than five seconds and minimum amplitude. Figure 8 shows the dynamic responses of $\Delta\omega$ for nominal operating conditions by Lead-Lag controller with ΔQ_e, ΔP_e and $\Delta P_e + \Delta Q_e$ input control signal. By comparing the above figures with those obtained by the controller with $\Delta\omega$ input in Figure 11.b, it can be seen that the response quality of ΔQ_e, ΔP_e, $\Delta P_e + \Delta Q_e$ based controller is less than $\Delta\omega$ based controller in terms of peak amplitude. Therefore it has been used from $\Delta\omega$ input signal for LQR and adaptive controller designing.

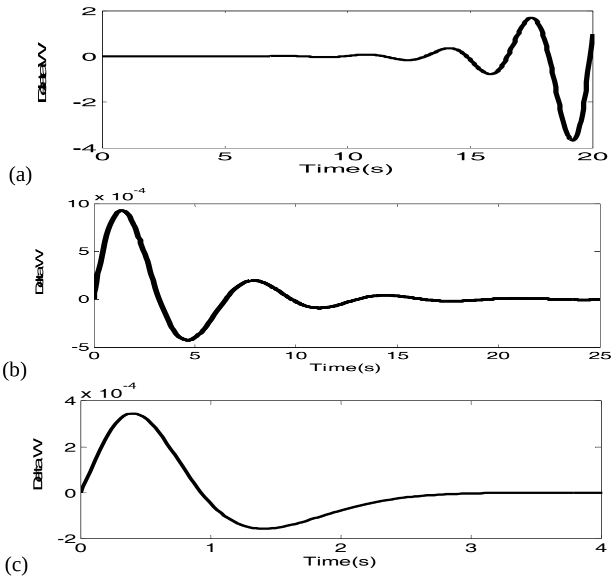

Figure 8. Dynamic responses of $\Delta\omega$ at nominal operating conditions for different input control signal
(a): ΔQ_e (b): ΔP_e (c): $\Delta P_e + \Delta Q_e$

Figure 9 shows the dynamic responses of $\Delta\omega$ at nominal condition with LQR damping controller versus $\Delta P_m = 0.01$pu perturbation of input mechanical power.

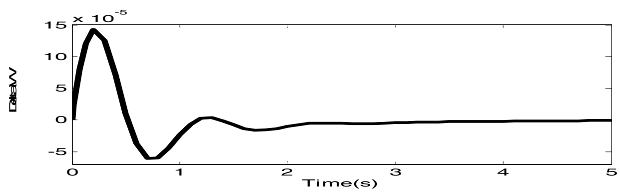

Figure 9. The dynamic responses of $\Delta\omega$ at nominal condition with LQR damping controller

Dynamic response has nearly the same quality in comparison with the Lead-Lag controller at Figure 7 (b) in terms of settling time and peak amplitude.

VI. CONCLUSIONS

In this paper, a UPFC has been used for dynamic stability improvement and state-space equations have been applied for the design of damping controllers. Simulation results operated by MATLAB/SIMULINK show that using an input speed deviation signal is better than inputs of power deviations, and also adding control signals to the active power control loop of the shunt inverter decreases speed oscillations effectively. According to the simulation results, the designed LQR controller for the system has the perfect effect in oscillation damping and dynamic stability improvement.

APPENDICES

Appendix 1. Test System Parameters

Generator:

$M = 2H = 8.0$MJ/MVA , $D = 0.0$

$X'_d = 0.3$pu $T'_{do} = 5.044$s $X_d = 1.0$pu $X_q = 0.6$pu

Excitation System:

$K_a = 100$ $T_a = 0.01$s

Transformer :

$X_{tE} = 0.1$pu $X_E = X_B = 0.1$pu $X_E = X_B = 0.1$pu

Transmission Line:

$X_{BV} = 0.3$pu $X_e = X_{BV} + X_B + X_{tE} = 0.5$pu

Operating Condition:

$V_t = 1.0$pu $P_e = 0.8$pu $V_b = 1.0$pu $f = 60$Hz

Parameters of DC Link:

$V_{dc} = 2$pu $C_{dc} = 1$pu

Appendix 2. *K*-Parameters of ΔQ_e Calculation

$$K_{10} = (-2x_q L)(x_{qE} + x_{qt})V_b \cos\delta / x_{q\Sigma} + $$
$$+E'_q V_b \sin\delta((x_{dE} - x_{dt}) / x_{d\Sigma})(2x'_d S + 1)$$
$$K_{11} = ((x_{BB} - x_E) / x_{d\Sigma})(2x'_d S - E'_q) - S$$
$$K_{12} = 2x_q L((x_{Bq} - x_{qE})\cos\delta_E m_E / 2x_{q\Sigma} + $$
$$+(x_{qt} - x_{qE})\cos\delta_B m_B / 2x_{q\Sigma}) + $$
$$+(2x'_d L - E'_q)((x_{dE} - x_{Bd})\sin\delta_E m_E / 2x_{d\Sigma} + $$
$$+(x_{dE} - x_{dt})\sin\delta_B m_B / 2x_{d\Sigma})$$
$$K_{13} = 2x_q L((x_{Bq} - x_{qE})\cos\delta_E V_{dc} / 2x_{q\Sigma} + $$
$$+(2x'_d S - E'_q)((x_{dE} - x_{Bd})\sin\delta_E V_{dc} / 2x_{d\Sigma})$$
$$K_{14} = 2x_q L((x_{Bq} + x_{qE})\sin\delta_E V_{dc} m_E / 2x_{q\Sigma} + $$
$$+(2x'_d S - E'_q)((x_{dE} - x_{Bd})\cos\delta_E V_{dc} m_E / 2x_{d\Sigma})$$
$$K_{15} = 2x_q L((x_{qt} - x_{qE})\cos\delta_B V_{dc} / 2x_{q\Sigma} + $$
$$+(2x'_d S - E'_q)((x_{dE} - x_{dt})\sin\delta_B V_{dc} / 2x_{d\Sigma})$$
$$K_{16} = 2x_q L((x_{qE} - x_{qt})\sin\delta_B V_{dc} m_B / 2x_{q\Sigma} + $$
$$+(2x'_d S - E'_q)((x_{dE} - x_{dt})\cos\delta_B V_{dc} m_B / 2x_{d\Sigma})$$

Appendix 3. *K*-Parameters for UPFC HVDC Network

$$K_1 = \frac{(V_{td} - I_{tq}x'_d)(x_{dE} - x_{dt})V_b \sin\delta}{x_{d\Sigma}} + \frac{(x_q I_{td} + V_{tq})(x_{qt} - x_{qE})V_b \cos\delta}{x_{q\Sigma}}$$

$$K_2 = \frac{-(x_{BB}+x_E)V_{td}}{x_{d\Sigma}x_d} + \frac{(x_{BB}+x_E)x'_d I_{tq}}{x_{d\Sigma}}$$

$$K_3 = 1 + \frac{(x'_d - x_d)(x_{BB}+x_E)}{x_{d\Sigma}}$$

$$K_4 = -\frac{(x'_d - x_d)(x_{dE}-x_{dt})V_b \sin\delta}{x_{d\Sigma}}$$

$$K_5 = \frac{V_{td}x_q(x_{qt}-x_{qE})V_b\cos\delta}{V_t x_{q\Sigma}} - \frac{V_{tq}x'_d(x_{dtE}-x_{dt})V_b\sin\delta}{V_t x_{d\Sigma}}$$

$$K_6 = \frac{V_{tq}(x_{d\Sigma}+x'_d(x_{BB}+x_E))}{V_t x_{d\Sigma}}$$

$$K_7 = 0.25C_{dc}(V_b \sin\delta(m_E\cos\delta_E x_{dE} - m_B\cos\delta_B x_{dt})) -$$
$$\frac{m_B\cos\delta_B x_{dt}}{x_{d\Sigma}} +$$
$$V_b\cos\delta(m_B\sin\delta_B x_{qt} - m_E\sin\delta_E x_{qe}$$

$$K_8 = -0.25\frac{m_B\cos\delta_B x_E + m_E\cos\delta_E x_{BB}}{x_{d\Sigma}}$$

$$K_9 = 0.25Cdc(\frac{m_B\sin\delta_B(m_B\cos\delta_B x_{dt} - m_E\cos\delta_E x_{dE})}{2x_{d\Sigma}} +$$
$$\frac{m_E\sin\delta_E(m_E\cos\delta_E x_{Bd} - m_B\cos\delta_B x_{dt})}{2x_{d\Sigma}}$$
$$\frac{m_B\cos\delta_B(m_B\sin\delta_B x_{qt} - m_E\sin\delta_E x_{qE})}{2x_{q\Sigma}} +$$
$$\frac{m_E\cos\delta_E(-m_B\sin\delta_B x_{qE} + m_E\sin\delta_E x_{Bq})}{2x_{q\Sigma}})$$

$$K_{pe} = \frac{(V_{td} - I_{tq}x'_d)(x_{Bd}-x_{dE})V_{dc}\sin\delta_E}{2x_{d\Sigma}} +$$
$$\frac{(x_q I_{td} + V_{tq})(x_{Bq}-x_{qE})V_{dc}\cos\delta_E}{2x_{q\Sigma}}$$

$$K_{p\delta E} = \frac{(V_{td} - I_{tq}x'_d)(x_{Bd}-x_{dE})V_{dc}m_E\cos\delta_E}{2x_{d\Sigma}} +$$
$$\frac{(x_q I_{td} + V_{tq})(-x_{Bq}+x_{qE})V_{dc}m_E\sin\delta_E}{2x_{q\Sigma}}$$

$$K_{pb} = \frac{(V_{td} - I_{tq}x'_d)(x_{dt}-x_{dE})x_{dc}\sin\delta_B}{2x_{d\Sigma}} +$$
$$\frac{(x_q I_{td} + V_{tq})(x_{qt}-x_{qE})V_{dc}\cos\delta_B}{2x_{q\Sigma}}$$

$$K_{p\delta B} = \frac{(V_{td} - I_{tq}x'_d)(x_{dE}+x_{dt})V_{dc}m_B\cos\delta_B}{2x_{d\Sigma}} +$$
$$\frac{(x_q I_{td} + V_{tq})(-x_{qt}+x_{qE})V_{dc}m_B\sin\delta_B}{2x_{q\Sigma}}$$

$$K_{qe} = -\frac{(x'_d - x_d)(x_{Bd}-x_{dE})V_{dc}\sin\delta_E}{2x_{d\Sigma}}$$

$$K_{q\delta e} = -\frac{(x'_d - x_d)(x_{Bd}-x_{dE})m_E V_{dc}\cos\delta_E}{2x_{d\Sigma}}$$

$$K_{qb} = -\frac{(x'_d - x_d)(x_{dt}-x_{dE})V_{dc}\sin\delta_B}{2x_{d\Sigma}}$$

$$K_{pd} = (V_{td} - I_{tq}x'_d)(\frac{(x_{dt}-x_{dE})m_B\sin\delta_B}{2x_{d\Sigma}} +$$
$$\frac{(x_{Bd}-x_{dE})m_E\sin\delta_E}{2x_{d\Sigma}}) +$$
$$(x_q I_{td} + V_{tq})(\frac{(x_{qt}-x_{qE})m_B\cos\delta_B}{2x_{q\Sigma}} +$$
$$\frac{(x_{Bq}-x_{qE})m_E\cos\delta_E}{2x_{q\Sigma}}$$

$$K_{q\delta B} = -\frac{(x'_d - x_d)(x_{dE}-x_{dt})m_B V_{dc}\cos\delta_B}{2x_{\Sigma}}$$

$$K_{qe} = -(x'_d - x_d)(\frac{(x_{Bd}-x_{dE})m_E\sin\delta_E}{2x_{d\Sigma}} + \frac{(x_{dt}-x_{dE})m_B\sin\delta_B}{2x_{d\Sigma}})$$

$$K_{ve} = \frac{V_{td}(x_{Bq}-x_{qE})V_{dc}\cos\delta_E}{2V_t x_{q\Sigma}} - \frac{V_{tq}(x_{Bd}-x_{dE})V_{dc}\sin\delta_E}{2V_t x_{d\Sigma}}$$

$$K_{v\delta E} = \frac{V_{td}x_q(x_{qE}-x_{Bq})m_E V_{dc}\sin\delta_E}{2V_t x_{q\Sigma}} - \frac{V_{tq}x'_d(x_{Bd}-x_{dE})m_E V_{dc}\cos\delta_E}{2V_t x_{q\Sigma}}$$

$$K_{vb} = \frac{V_{td}x_q(x_{qt}-x_{qE})V_{dc}\cos\delta_E}{2V_t x_{q\Sigma}} - \frac{V_{tq}x'_d(x_{dt}-x_{dE})V_{dc}\sin\delta_E}{2V_t x_{d\Sigma}}$$

$$K_{v\delta B} = \frac{V_{td}x_q(x_{qE}-x_{qt})m_B V_{dc}\sin\delta_E}{2V_t x_{q\Sigma}} + \frac{V_{tq}m_B x'_d(x_{dE}+x_{dt})V_{dc}\cos\delta_E}{2V_t x_{d\Sigma}}$$

$$K_{vd} = \frac{V_{td}x_q(x_{Bq}-x_{qE})m_E\cos\delta_E}{2V_t x_{q\Sigma}} + \frac{(x_{qt}-x_{qE})m_B\cos\delta_B}{2x_{q\Sigma}} -$$
$$\frac{V_{tq}m_E x'_d(x_{Bd}-x_{dE})\sin\delta_E}{2V_t x_{d\Sigma}} + \frac{m_B(x_{dt}-x_{qE})\sin\delta_E}{2x_{d\Sigma}}$$

$$K_{ce} = 0.25C_{dc}\frac{V_{dc}\sin\delta_E(m_E\cos\delta_E x_{Bd} - m_B\cos\delta_B x_{dE})}{2x_{d\Sigma}} +$$
$$\frac{V_{dc}\cos\delta_E(m_E\sin\delta_E x_{Bq} - m_B\sin\delta_B x_{qE})}{2x_{q\Sigma}}$$

$$K_{c\delta e} = \frac{0.25m_E}{C_{dc}}(\cos\delta_E I_{Eq} - \sin\delta_E I_{Ed}) +$$
$$\frac{0.25}{C_{dc}}(m_E V_{dc}\cos\delta_E\frac{(m_E\cos\delta_E x_{Bd} - m_B\cos\delta_B x_{dE})}{2x_{d\Sigma}} +$$
$$m_E V_{dc}\sin\delta_E\frac{(m_B\sin\delta_B x_{qE} + m_E\sin\delta_E x_{Bq})}{2x_{q\Sigma}})$$

$$K_{cb} = 0.25C_{dc}\frac{V_{dc}\sin\delta_B(-m_E\cos\delta_E x_{dE} + m_B\cos\delta_B x_{dt})}{2x_{d\Sigma}} +$$
$$\frac{V_{dc}\cos\delta_B(m_B\sin\delta_E x_{qt} - m_E\sin\delta_E x_{qE})}{2x_{q\Sigma}}$$

$$K_{c\delta B} = \frac{0.25m_B}{C_{dc}}(\cos\delta_B I_{Bq} - \sin\delta_B I_{Bd}) +$$
$$\frac{0.25}{C_{dc}}(m_B V_{dc}\cos\delta_B\frac{(m_E\cos\delta_E x_{dE} + m_B\cos\delta_B x_{dt})}{2x_{d\Sigma}} +$$
$$m_B V_{dc}\sin\delta_B\frac{(-m_B\sin\delta_E x_{qt} + m_E\sin\delta_E x_{qE})}{2x_{q\Sigma}})$$

REFERENCES

[1] H.F. Wang, "Damping Function of Unified Power Flow Controller", IEE Proc. Gen. Trans. and Distrib., Vol. 146, No. 1, pp. 81-87, January 1999.
[2] C. Qin, W.J. Du, H.F. Wang, Q. Xu, P. Ju, "Controllable Parameter Region and Variable-Parameter Design of Decoupling Unified Power Flow Controller", Transmission and Distribution Conference and Exhibition, Asia and Pacific, IEEE/PES, Dalian, China, 2005.
[3] H.F. Wang, "Damping Function of Unified Power Flow Controller", IEE Proc. Gen. Trans. and Distrib., Vol. 146, No. 1, pp. 81-87, 1999.
[4] M.A. Abido, A.T. Al-Awami, Y.L. Abdel-Magid, "Simultaneous Design of Damping Controllers and Internal Controllers of a Unified Power Flow Controller", IEEE Power Engineering Society General Meeting, Montreal, Canada, 2006.
[5] C.M. Yam, M.H. Haque, "A SVD Based Controller of UPFC for Power Flow Control", The 15th Power System Computation Conference, Session 12, pp. 2, 1-7 August 2005.
[6] M.A. Abido, "Particle Swarm Optimization for Multimachine Power System Stabilizer Design", IEEE Power Engineering Society Summer Meeting, Vol. 3, 15-19, pp. 1346-1351, July 2001.
[7] H.F. Wang, "Application of Modeling UPFC into Multi-Machine Power Systems", IEE Proc. Gen. Trans. and Distrib., Vol. 146, No. 3, pp. 306-312, 1999.
[8] A. Nabavi-Niaki, M.R. Iravani, "Steady-State and Dynamic Models of Unified Power Flow Controller (UPFC) for Power System Studies", IEEE Transactions on Power Systems, Vol. 11, No. 4, pp. 1937-1943, Nov. 1996.
[9] R.P. Kalyani, G.K. Venayagamoorthy, "Two Separately Continually Online Trained Neurocontrollers for a Unified Power Flow Controller", International Conference on Intelligent sensing and Information processing, IEEE Cat. No. 04EX783, pp. 243-248, 2004.
[10] A.J.F. Keri, X. Lombard, A.A. Edris, "Unified Power Flow Controller: Modeling and Analysis", IEEE Transactions on Power Delivery, Vol. 14, No. 2, pp. 648-654, April 1999.
[11] H.F. Wang, "Application of Modeling UPFC into Multi-Machine Power System", IEE Proc. Gen. Trans. and Distrib., Vol. 146, No. 3, pp. 306-312, 1999.
[12] L. Rouco, "Coordinated Design of Multiple Controllers for Damping Power System Oscillation", Electric Power Energy Systems, 21, pp. 517-530.
[13] B.C. Pal, "Robust Damping of Interarea Oscillations with Unified Power Flow Controller", IEE Proc. Gen. Trans. and Distrib., Vol. 149, No. 6, pp.733-738, 2002.
[14] D. Nazarpour, S.H. Hosseini, G.B. Gharehpetian, "An Adaptive STATCOM Based Stabilizer for Damping Generator Oscillations", ELECO Conference, Bursa, Turkey, pp. 60-64, 7-11 December 2005.
[15] C.H. Cheng, Y.Y. Hsu, "Damping of Generator Oscillations Using an Adaptive Static VAR Compensator", IEEE Transactions on Power Systems, Vol. 7, No. 2, May 1992.
[16] H. Shayeghi, H.A. Shayanfar, F. Shalchi, "Robust Loop-Shaping based POD Controller Design for UPFC", Internatioal Journal on Technical and Physical Problems of Engineering (IJTPE), Issue 3, Vol. 2, No. 2, pp. 45-51, June 2010.
[17] N.M. Tabatabaei, A. Hashemi, N. Taheri, F.M. Sadikoglu, "A Novel on Line Adaptive based Stabilizer for Dynamic Stability Improvement with UPFC", Internatioal Journal on Technical and Physical Problems of Engineering (IJTPE), Issue 8, Vol. 3, No. 3, pp. 93-99, September 2011.

BIOGRAPHIES

Naser Mahdavi Tabatabaei was born in Tehran, Iran, 1967. He received the B.Sc. and the M.Sc. degrees from University of Tabriz (Tabriz, Iran) and the Ph.D. degree from Iran University of Science and Technology (Tehran, Iran), all in Power Electrical Engineering, in 1989, 1992, and 1997, respectively. Currently, he is a Professor of Power Electrical Engineering at International Ecoenergy Academy, International Science and Education Center and International Organization on TPE (IOTPE). He is also an academic member of Power Electrical Engineering at Seraj Higher Education Institute and teaches Power System Analysis, Power System Operation, and Reactive Power Control. He is the secretary of International Conference on TPE (ICTPE), editor-in-chief of International Journal on TPE (IJTPE) and chairman of International Enterprise on TPE (IETPE) all supported by IOTPE. His research interests are in the area of power quality, energy management systems, ICT in power engineering and virtual e-learning educational systems. He is a member of the Iranian Association of Electrical and Electronic Engineers (IAEEE).

Aysen Demiroren was born in Bursa, Turkey, 1959. She received her B.Sc. and M.Sc. degrees of Electrical Engineering from Istanbul Technical University (Istanbul, Turkey) in 1982, and 1985, respectively. From 1985 to 1993 she was a doctoral student at the Institute of Science and Technology, Istanbul Technical University and received Ph.D. degree in 1993. Her Ph.D. thesis was related to Adaptive Control of Synchronous Machine. She was an Assistant Professor from 1993 to 1996 and an Associate Professor from 1996 to 2003 at the Department of Electrical Engineering, Faculty of Electrical and Electronics Engineering, Istanbul Technical University. She has been Professor since 2003 at the same department. Her research interests are power system control and modern control techniques, electrical energy generation, renewable energy sources.

Naser Taheri was born in Iran. He received his B.Sc. from University of Guilan, (Rasht, Iran) in Electronic Engineering, 2007 and M.Sc. degree from Azarbaijan University of Tarbiat Moallem (Tabriz, Iran) in Power Electrical Engineering, 2009. He is currently researching on power system control, flexible AC transmission systems (FACTS) and power systems dynamic modeling.

Ahmad Hashemi was born in Kermanshah, Iran, 1984. He received his B.Sc. degree in Power Electrical Engineering from K.N. Toosi University of Technology (Tehran, Iran) in 2006 and M.Sc. degree from Azarbaijan University of Tarbiat Moallem (Tabriz, Iran) in 2009. His main research interests are FACTS devices modeling, adaptive control, neural network optimizations, system operation, and reactive power control.

Narges Sadat Boushehri was born in Iran. She received her B.Sc. from Sharif University of Technology (Tehran, Iran) in Control Engineering and Islamic Azad University, Central Tehran Branch (Tehran, Iran) in Electronic Engineering, 1991 and 1996 and the M.Sc. degree from International Ecocenergy Academy (Baku, Azerbaijan) in Electronic Engineering, 2009. She is currently researching on power system control and artificial intelligent algorithms.